Published in final edited form as:
Langmuir. 2013 August 6; 29(31): 9891–9896. doi:10.1021/la401891f.

PEG-Stabilized Core–Shell Surface-Imprinted Nanoparticles

Ewa Moczko, **Antonio Guerreiro**, **Elena Piletska**, and **Sergey Piletsky**
Cranfield Health, Cranfield University, Cranfield, Bedfordshire MK43 0AL, U.K.

Abstract

Here we present a simple technique to produce target-specific molecularly imprinted polymeric nanoparticles (MIP NPs) and their surface modification in order to prevent the aggregation process that is ever-present in most nanomaterial suspensions/dispersions. Specifically, we studied the influence of surface modification of MIP NPs with polymerizable poly(ethylene glycol) on their degree of stability in water, in phosphate buffer, and in the presence of serum proteins. Grafting a polymer shell on the surface of nanoparticles decreases the surface energy, enhances the polarity, and as a result improves the dispersibility, storage, and colloidal stability as compared to those of core (unmodified) particles. Because of the unique solid-phase approach used for synthesis, the binding sites of MIP NPs are protected during grafting, and the recognition properties of nanoparticles are not affected. These results are significant for developing nanomaterials with selective molecular recognition, increased biocompatibility, and stability in solution. Materials synthesized this way have the potential to be used in a variety of technological fields, including in vivo applications such as drug delivery and imaging.

Introduction

Research associated with the development of smart materials operating on the nanometer scale is a rapidly growing field.[1-4] Nanoparticles can offer significant advantages because of their size, perceived dispersibility, and high external surface area to volume ratio. Additionally, their unique properties can be easily controlled and modified to address the requirements of specific applications. Among these are ultrasensitive clinical and environmental sensors, biomedical imaging, drug delivery, and novel therapeutic agents.[5-10] The stability and behavior of nanoparticles, both in vitro and in vivo, are strongly related to their physical and chemical properties such as size, shape, and surface characteristics (e.g., hydrophobicity, biocompatibility, charge).[11, 12] Additionally, because of high surface energies, solutions of nanoparticles are thermodynamically unstable and tend to form aggregates over time. This can seriously affect the performance and usefulness of nanoparticle preparations by restricting access to binding sites, resulting in poor rheology or precipitation from solution. This is of special concern for potential in vivo applications, where the formation of aggregates/flocculation can be particularly problematic.

One of the most common methods for preventing nanoparticle aggregation is steric stabilization, which can be performed by modifying their surfaces and creating a physical barrier between them.(12) This can be achieved by grafting a suitable polymeric layer to the surface of nanoparticles, which improves their dispersion and solubility.[13-15]

Europe PMC Funders Author Manuscripts

Europe PMC Funders Author Manuscripts

Here we describe the synthesis of robust and highly selective polymeric nanoparticles and their surface modification with poly(ethylene glycol) (PEG) derivatives in order to improve their biocompatibility and stability in solution.[16-18] Steps in the synthesis of core–shell MIP NPs are presented schematically in Figure 1.

A polymerization mixture comprising functional monomer, cross-linker, initiator (iniferter), and solvent was loaded onto the solid phase with a previously immobilized template. Then polymerization was initiated using UV irradiation. After synthesis, nonreacted monomers and low-affinity particles were eluted from the solid phase at low temperature while the high-affinity NPs remained bound to the template. They were subsequently grafted by the addition of a solution of polymerizable PEG to the solid phase containing the bound-core NPs and reapplying UV light. After the polymerization of the shell and further washing, the temperature of the solvent was increased, allowing the elution of the high-affinity core–shell MIP NPs with high solution stability.

Materials and Methods

Materials

Melamine (MEL), desisopropyl atrazine (DA), methacrylic acid (MAA), ethylene glycol dimethacrylate (EGDMA), trimethylolpropane trimethacrylate (TRIM), pentaerythritol-tetrakis-(3-mercaptopropionate) (PETMP), phosphate-buffered saline (PBS), glutaraldehyde (GA), poly(ethylene glycol) methacrylate (PEG, Mw = 360 g mol^{-1}), poly(ethylene glycol) methacrylate (PEG, Mw = 1100 g mol−1), solid glass beads (75 μm diameter), and bovine serum albumin (BSA) were purchased from Sigma-Aldrich, U.K. Acetonitrile (ACN), ethanol, methanol, and acetone were purchased from VWR (U.K.). Sodium hydroxide and hydrochloric acid were obtained from Fisher Scientific (U.K.). N,N-Diethyldithiocarbamic acid benzyl ester was purchased from TCI Europe (Belgium). Deionized water obtained from a Millipore (Milli-Q) purification system at a resistivity of 18.2 MΩ cm was used for analysis. All chemicals were analytical or HPLC grade and were used without further purification.

Synthesis and Postderivatization of Melamine MIP NPs

The protocol for solid-phase preparation with an immobilized template for the synthesis of MIP nanoparticles was adopted from Moczko et al.[19] The composition of the polymerization mixture for the synthesis of the core MIP NPs for melamine detection was adapted from Guerreiro et al. and Poma et al. [17, 20] A monomer mixture was prepared by mixing MAA (2.88 g) as a functional monomer, EGDMA (3.24 g) and TRIM (3.24 g) as cross-linkers, N,N-diethyldithiocarbamic acid benzyl ester (0.753 g) as an iniferter, and pentaerythritol-tetrakis-(3-mercaptopropionate) (PETMP) (0.18 g) as a chain-transfer agent. All compounds were dissolved in ACN (10.52 g). The mixture was placed in a glass vial and purged with N_2 for 20 min. Melamine-derivatized glass beads (solid phase, 30 g), prepared as previously described,[19] were placed in a 200 mL flat-bottomed glass beaker and degassed in vacuo for 20 min. The polymerization mixture was poured onto the solid phase, and the vessel was then placed between two UV light sources (Philips model HB/171/A, each fitted with 4 × 15 W lamps) for 1 min under a continuous stream of nitrogen. After

polymerization, the contents of the beaker ware transferred to an SPE cartridge fitted with a polyethylene frit (20 μm porosity) in order to perform the temperature-based affinity separation of MIP NPs. The temperature of ACN and the SPE cartridge was kept at 20 °C. Washing was performed with 10 bed volumes of ACN (relative to the volume of the solid phase). This was done in order to remove nonpolymerized monomers and low-affinity polymer. The effectiveness of the washing was verified by measuring the UV absorbance of washing aliquots in order to ensure complete monomer removal. After the cold washing step and before the high-temperature elution, high-affinity core NPs bound to the solid phase were derivatized. For this, different amounts of poly(ethylene glycol) methacrylate with either 360 or 1100 g mol^{-1} were dissolved in 7.5 mL of ACN and added to the solid phase with attached MIP NPs recovered from the SPE cartridge. The mixture was bubbled with N2 for 5 min and irradiated with UV for 1 min 30 s using the same arrangement of lamps as described above. Following irradiation, the contents were again transferred to an SPE cartridge and the solid phase was washed with 10 bed volumes of ACN at 20 °C.

After washing at low temperature, the SPE cartridge containing the beads and the core–shell NPs was conditioned at 60 °C and washed with hot ACN at 60 °C (six bed volumes). The total volume of the collected solution of high-affinity core–shell MIP NPs in ACN was 100 mL.

Dynamic Light Scattering (DLS)

Particles sizes were measured with a Zetasizer Nano (Nano-S) particle-size analyzer from Malvern Instruments Ltd. (U.K.). Samples were prepared by dissolving 150 μL of stock NPs in water (at a concentration of 0.1 nM) in 1.5 mL of PBS buffer and sonicating for 5 min. In later experiments, 100 μL of BSA (80 mg/mL, 80 × 103 ppm) was added to the NP suspension. The degree of particle aggregation was analyzed by DLS at 25 °C in a 3 cm^3 disposable polystyrene cuvette. Each value is reported as the average of at least three measurements.

Transmission Electron Microscopy (TEM) Analysis

TEM images were obtained using a Philips CM20 transmission electron microscope. Prior to TEM analysis, samples were sonicated for 1 min before a drop of the sample was placed on a carbon-coated copper grid and dried in air.

Static Water Contact Angle Measurements

A film of NPs was prepared on a glass slide by the evaporation of 100 μL of a solution of nanoparticles at 60 °C. The static water contact angle was then measured on the surface of the film using a Cam 100 optical angle meter (KSV Instruments Ltd., Finland) along with the software provided.

Determination of Zeta Potential

Solutions of nanoparticles in water were analyzed using a Zetasizer 3000 (Malvern Instruments, U.K.).

Surface Plasmon Resonance (SPR)

SPR experiments were carried out using a Biacore 3000 SPR system (GE Healthcare Life Sciences, U.K.) Au-coated chips (SIA Kit Au, Biacore), purchased from GE Healthcare Life Science (U.K.), were cleaned by immersion in piranha solution (3:1 v/v H_2SO_4/H_2O_2) for 5 min, thoroughly rinsed with deionized water, and left in ethanol overnight. The immobilization of the templates was performed by incubating the chips in a solution of cysteamine (0.2 mg mL^{-1} in ethanol) at 4 °C for 24 h, after which they were washed with ethanol and incubated in a 7% v/v solution of GA in PBS pH 7.4 for 2 h. After this step, the chips were washed with PBS and immersed in a solution of MEL or DA (1.2 mg mL^{-1}) in PBS pH 7.4 containing 20% v/v methanol as a cosolvent for 24 h at 4 °C. Afterwards, chips were washed with methanol and dried in air. Once the immobilization was completed, the chips were assembled on their holders and stored under Ar at 4 °C until they were used. A volume of nanoparticle solution in ACN (10 mL) was first concentrated down to about 5 mL and twice diluted with water and then concentrated down again to 5 mL by evaporation of the solvent and used to prepare stock solutions of NPs for injection. This was done in order to remove most of the ACN. The molar concentration of NPs was determined as described previously.(20, 21) The interaction analysis was performed at 25 and 36 °C using PBS (0.01 M potassium phosphate, 0.0027 M potassium chloride, and 0.137 M sodium chloride, pH 7.4) as the running buffer at a flow rate of 15 μL min^{-1}. The aqueous stock suspensions of the NPs were filtered through PTFE syringe filters with a pore diameter of 0.45 μm (Supelco, U.K.) and diluted in PBS for the analysis following a series of 2-fold dilutions. The range of concentrations of nonmodified NPs was from 0.003 to 1.84 nM, and the concentration range of PEG-NPs was from 0.0056 to 1.45 nM. Sensorgrams were collected sequentially for all analyte concentrations running in KINJECT mode (injection volume, 100 μL; dissociation time, 120 s). Dissociation constants (KD) were calculated from plots of the equilibrium biosensor response using the BiaEvaluation v4.1 software with a 1:1 binding model with drifting baseline fitting.

Results and Discussion

The synthesis of core–shell MIP NPs was performed using a protocol and procedures adapted from Guerreiro et al., Poma et al., and Moczko et al.[17, 19, 20] Nanoparticles were imprinted against melamine (MEL), which can form strong electrostatic bonds with functional monomer methacrylic acid.[17, 22] MEL was selected as a demonstration target, although the main aim of the work was to study the effects of the PEG shell on the aggregation profile of NP. Because grafting can interfere with the recognition properties of the synthesized core–shell NP, it was important to produce imprinted materials and therefore verify if the presence of the immobilized template was in fact protecting the binding region during the formation of the shell. Polymerization was initiated by a living initiator, which enables polymer chains to grow at a controlled rate, prevents side reactions, and thus facilitates the creation of good imprints during synthesis.[23] This and the short irradiation time result in the formation of small, homogeneous nanoparticles with a high affinity for the template.[17, 24-27] Another advantage of this approach is the ability to reinitiate polymerization by UV irradiation using macroiniferter moieties present on the surfaces of the nanoparticles.[23, 28] This approach was used together with the introduction of a

secondary monomer (PEG-methacrylate) to graft the shell whereas the high-affinity particles were still attached to the template and binding sites were protected from modification. The presence of PEG was confirmed by NMR measurements[19] and visualized using TEM analysis. A typical TEM picture of dry MIP nanoparticles is presented in Figure 2, which clearly shows their core–shell structure. The size distribution of NPs was calculated using DLS, which allows the analysis of the NP suspension in solution. The average hydrodynamic diameters of the core (unmodified) and core–shell MIP NPs in water were approximately 105 ± 4 and 109 ± 12 nm, respectively, which proves their nanoscale sizes. Although the small size of the core NPs makes them attractive materials for a number of practical applications, it also brings in the aforementioned disadvantages (high surface energy, enhanced reactivity, and tendency toward aggregation). This not only decreases the stability of NPs in suspension but also reduces the shelf life of any product containing NPs and therefore limits the scope of most practical applications. Coating the core NPs with a hydrophilic polymer shell such as PEG has previously been suggested as one way to stabilize them against aggregation and render them more suitable for in vitro or in vivo applications.[1, 29-31]

The main objective of these studies was to investigate the influence of the surface modification of imprinted nanoparticles on their performance in terms of stability in aqueous media and recognition properties. In this study, MIP NPs were grafted with different amounts of two types of polymerizable PEGs (lower-molecular-weight PEG methacrylate 360 and PEG methacrylate 1100). The measurements were carried out in deionized water, in PBS at different pH values, and also in the presence or absence of serum albumin (BSA). They were performed in order to simulate the physiological environment and to compare the behavior of nanoparticles under different conditions. The degree of particle aggregation was monitored on a daily basis using DLS.

An initial assessment of the performance of the two PEGs was carried out in order to select the one that yielded the best results in terms of the potential for reducing particle aggregation; the results are summarized in Figure 3. It shows changes in the diameters of core and modified MIP NPs in response to their storage conditions at different pH values in PBS buffer. The presence of a shell of PEG 1100 clearly improves the stability of NPs in solution, especially at lower pH. This can possibly be attributed to the increased degree of protonation of the carboxylate groups of the monomer, resulting in reduced charge repulsion between particles and consequently increased aggregation. Contact angle measurements performed on dry nanoparticle films indicate a considerable increase in the hydrophilicity of the surface and consequently of the NPs once grafted with either PEG. Films prepared with core NPs had a water contact angle of 59.8 ± 1.6°, and films prepared with core–shell NPs grafted with PEG 360 and PEG 1100 had water contact angles of 45.4 ± 11.5 and 32.9 ± 2.2°, respectively. The results are consistent with the obtained aggregation data (Figure 3), where the more polar core–shell NPs prepared with longer PEG possess increased stability in solution.

Accordingly, PEG methacrylate 1100 was selected as the best monomer because of better aggregation-prevention properties. Additional studies were performed in order to optimize the amount of PEG 1100 used to produce the shell. This included testing the NP aggregation

profile over time at different pH values in PBS buffer (Figure 4). The best solution stability was obtained when core–shell NPs were synthesized with 10 mg mL^{-1} (75 mg in 7.5 mL) PEG 1100. Accordingly, these NPs were used in all subsequent experiments as described from here onward and described as MIP NPs PEG 1100 75.

Promising results were also obtained when the long-term stability of NPs was assessed in deionized water (Figure 5). Data points on the graph indicate how the average hydrodynamic diameter changed over time. A clear increase in the apparent size of core (unmodified) MIP NPs can be observed after about 288 h or 12 days (triangles), indicating the presence of the aggregation processes. This trend is absent for particles modified by the hydrophilic shell of PEG 1100 grafted to their surface, which significantly reduces the rate of aggregation and therefore would suggest an improvement in stability when NPs are dispersed in water (circles).

According to zeta potential measurements, both core and core–shell nanoparticles have a negative potential, which can be attributed to the presence of charged carboxylic moieties. MIP NP PEG 1100 are slightly more negative (−58.1 ± 1.5 mV) when compared to core MIP NPs, with a potential of −43.0 ± 0.8 mV. This can be explained by better wetting and improved water accessibility to the ionic groups of the polymer once it is grafted with a hydrophilic shell. In addition to steric effects of the hydrophilic shell, the higher potential might also contribute to the observed colloidal stability of core–shell NPs. Further tests were performed in order to investigate the effect of the presence of serum proteins on particle aggregation. This was done in order to assess the potential for in vivo and also diagnostic applications, where proteins are likely to be present at high concentration. The results in Figure 6 show that presence of protein in solution significantly reduces their aggregation, which might be explained by the fact that proteins adsorbed onto the particle surface create a hydrophilic layer/coating that ultimately stabilizes the suspension of NPs, even if the presence of the PEG shell leads to decreased protein adsorption.(32, 33) Furthermore, the presence of the hydrophilic PEG shell still appears to result in an improved aggregation profile, with practically no aggregation detected at physiological pH (pH 7.4).

To confirm if the molecular recognition properties of the core–shell NP remained unaffected by the grafting process, surface plasmon resonance (SPR) tests were performed. The affinity and selectivity of melamine core and core–shell NPs were compared using sensor surfaces modified with MEL (template) and a structural analogue, desisopropyl atrazine (DA) (Figure 7a,b, respectively), for the respective SPR sensorgrams. This procedure was adapted from Hosino et al. and Poma et al., who measured and quantified binding interactions of imprinted NPs onto surfaces containing immobilized template molecules.(20, 21) Measurements were performed at 25 °C and also at 36 °C in order to simulate body temperature. The apparent dissociation constants (KD) for core MIP NPs and core–shell MIP NPs PEG 1100 75 on the specific and nonspecific surfaces at 25 and 36 °C are presented in Table 1. The results show that lowest KD values were obtained at 25 °C for both types of particles on the MEL surface and are within the same order of magnitude even at 36 °C. On specificity tests, the KD values obtained for both particles on the DA surface are much greater (at least 2 orders of magnitude) and are outside the range of concentrations of NPs tested (from 0.0056 to 1.45 nM). Consequently, experimental data cannot be

correctly fitted with the BiaEvaluation software; therefore, KD cannot be accurately determined. Concentrations of NPs greater than 1.5–1.6 nM could not be prepared because of solubility issues, with the appearance of slight opalescence, and so were unsuitable for SPR analysis. Nevertheless, the results confirm that the recognition properties of surface-imprinted NPs are not affected by the grafting of the PEG shell and that both types of NPs maintain their remarkable affinity and specificity at 36 °C.

Conclusions

The high surface energy of polymeric nanoparticles makes them generally unstable in solution and susceptible to self-aggregation, which over time might lead to precipitation. Here we present the detailed optimization of a method for the manufacture of core–shell MIP nanoparticles that significantly improved its solution stability without any additional stabilizers. This was achieved by grafting an optimal amount of hydrophilic PEG onto the surface of core MIP nanoparticles. Additionally, the surface modification did not affect the recognition properties of the nanoparticles because binding sites were effectively protected during shell synthesis by the template immobilized on a solid support. Further experiments indicate the stability of the nanoparticles in the presence of serum albumin and excellent affinity and specificity for the target molecule at both 25 and 36 °C. These results point toward the possibility of using the nanomaterials developed here as viable alternatives to biomolecules such as antibodies in a range of technological fields, including eventual in vivo applications.[34-36]

Acknowledgment

This work was supported by the Wellcome Trust with a Translation Award and by the Research Executive Agency (REA) of the European Union under grant agreement number PITN-GA-2010-264772 (ITN CHEBANA).

References

1. Doshi N, Mitragotri S. Designer biomaterials for nanomedicine. Adv. Funct. Mater. 2009; 19:3843–3854.
2. Ye L, Mosbach K. Molecular imprinting: synthetic materials as substitutes for biological antibodies and receptors. Chem. Mater. 2008; 20:859–868.
3. Wei SY, Wang Q, Zhu JH, Sun LY, Lin HF, Guo ZH. Multifunctional composite core-shell nanoparticles. Nanoscale. 2011; 3:4474–4502. [PubMed: 21984390]
4. Schartl W. Current directions in core-shell nanoparticle design. Nanoscale. 2010; 2:829–843. [PubMed: 20644772]
5. Parveen S, Misra R, Sahoo SK. Nanoparticles: a boon to drug delivery, therapeutics, diagnostics and imaging. Nanomed.-Nanotechnol. Biol. Med. 2012; 8:147–166.
6. Jain KK. Applications of nanobiotechnology in clinical diagnostics. Clin. Chem. 2007; 53:2002–2009. [PubMed: 17890442]
7. Diebold Y, Calonge M. Applications of nanoparticles in ophthalmology. Prog. Retin. Eye Res. 2010; 29:596–609. [PubMed: 20826225]
8. Tang D, Cui Y, Chen G. Nanoparticle-based immunoassays in the biomedical field. Analyst. 2013; 138:981–990. [PubMed: 23304696]
9. Wagh A, Qian SY, Law B. Development of biocompatible polymeric nanoparticles for in vivo NIR and FRET imaging. Bioconjugate Chem. 2012; 23:981–992.

10. Lipani E, Laurent S, Surin M, Vander Elst L, Leclére P, Muller RN. High-relaxivity and luminescent silica nanoparticles as multimodal agents for molecular imaging. Langmuir. 2013; 29:3419–3427. [PubMed: 23383648]
11. Nahar M, Dutta T, Murugesan S, Asthana A, Mishra D, Rajkumar V, Tare M, Saraf S, Jain NK. Functional polymeric nanoparticles: an efficient and promising tool for active delivery of bioactives. Crit. Rev. Ther. Drug Carrier Syst. 2006; 23:259–318. [PubMed: 17341200]
12. Albanese A, Tang PS, Chan WCW. The effect of nanoparticle size, shape, and surface chemistry on biological systems. Annu. Rev. Biomed. Eng. 2012; 14:1–16. [PubMed: 22524388]
13. Boyer C, Whittaker MR, Bulmus V, Liu JQ, Davis TP. The design and utility of polymer-stabilized iron-oxide nanoparticles for nanomedicine applications. NPG Asia Mater. 2010; 2:23–30.
14. Hafelli UO, Riffle JS, Harris-Shekhawat L, Carmichael-Baranauskas A, Mark F, Dailey JP, Bardenstein D. Cell uptake and in vitro toxicity of magnetic nanoparticles suitable for drug delivery Mol. Pharm. 2009; 6:1417–1428.
15. Thanh NTK, Green LAW. Functionalisation of nanoparticles for biomedical applications. Nano Today. 2010; 5:213–230.
16. Poma A, Turner APF, Piletsky SA. Advances in the manufacture of MIP nanoparticles. Trends Biotechnol. 2010; 28:629–637. [PubMed: 20880600]
17. Guerreiro AR, Chianella I, Piletska E, Whitcombe MJ, Piletsky SA. Selection of imprinted nanoparticles by affinity chromatography. Biosens. Bioelectron. 2009; 24:2740–2743. [PubMed: 19217769]
18. Vasapollo G, Del Sole R, Mergola L, Lazzoi MR, Scardino A, Scorrano S, Mele G. Molecularly imprinted polymers: present and future prospective. Int. J. Mol. Sci. 2011; 12:5908–5945. [PubMed: 22016636]
19. Moczko E, Poma A, Guerreiro A, Perez de Vargas Sansalvador I, Caygill S, Canfarotta F, Whitcombe MJ, Piletsky SA. Surface-modified multifunctional MIP nanoparticles. Nanoscale. 2013; 5:3733–3741. [PubMed: 23503559]
20. Poma A, Guerreiro A, Whitcombe MJ, Piletska EV, Turner APF, Piletsky SA. Solid-phase synthesis of molecularly imprinted polymer nanoparticles with a reusable template–"plastic antibodies. Adv. Funct. Mater. 2013; 23:2821–2827.
21. Hoshino Y, Kodama T, Okahata Y, Shea KJ. Peptide imprinted polymer nanoparticles: a plastic antibody. J. Am. Chem. Soc. 2008; 130:15242–15243. [PubMed: 18942788]
22. Li M, Zhang LY, Meng ZH, Wang ZY, Wu H. Molecularly-imprinted microspheres for selective extraction and determination of melamine in milk and feed using gas chromatography-mass spectrometry. J. Chromatogr., B. 2010; 878:2333–2338.
23. Kannurpatti AR, Lu SX, Bunker GM, Bowman CN. Kinetic and mechanistic studies of iniferter photopolymerizations. Macromolecules. 1996; 29:7310–7315.
24. Haupt K. Molecularly imprinted polymers: the next generation. Anal. Chem. 2003; 75:376A–383A.
25. Piletsky SA, Piletska EV, Karim K, Freebairn KW, Legge CH, Turner APF. Polymer cookery: influence of polymerization conditions on the performance of molecularly imprinted polymers. Macromolecules. 2002; 35:7499–7504.
26. Mijangos I, Navarro-Villoslada F, Guerreiro A, Piletska E, Chianella I, Karim K, Turner A, Piletsky S. Influence of initiator and different polymerisation conditions on performance of molecularly imprinted polymers. Biosens. Bioelectron. 2006; 22:381–387. [PubMed: 16782322]
27. Piletsky SA, Guerreiro A, Piletska EV, Chianella I, Karim K, Turner APF. Polymer cookery. 2. Influence of polymerization pressure and polymer swelling on the performance of molecularly imprinted polymers. Macromolecules. 2004; 37:5018–5022.
28. Otsu T. Iniferter concept and living radical polymerization. J. Polym. Sci., Polym. Chem. 2000; 38:2121–2136.
29. Carter SR, Rimmer S. Surface molecularly imprinted polymer core-shell particles. Adv. Funct. Mater. 2004; 14:553–561.
30. Rozenberg BA, Tenne R. Polymer-assisted fabrication of nanoparticles and nanocomposites. Prog. Polym. Sci. 2008; 33:40–112.

31. Otsuka H, Nagasaki Y, Kataoka K. PEGylated nanoparticles for biological and pharmaceutical applications. Adv. Drug Delivery Rev. 2003; 55:403–419.
32. Klein J. Probing the interactions of proteins and nanoparticles. Proc. Natl. Acad. Sci. U.S.A. 2007; 104:2029–2030. [PubMed: 17284585]
33. Cedervall T, Lynch I, Foy M, Berggård T, Donnelly S, Cagney G, Linse S, Dawson K. Detailed identification of plasma proteins adsorbed on copolymer nanoparticles. Angew. Chem., Int. Ed. 2007; 46:5754–5756.
34. Haupt K. Plastic antibodies. Nat. Mater. 2010; 9:612–614. [PubMed: 20651801]
35. Hoshino Y, Koide H, Urakami T, Kanazawa H, Kodama T, Oku N, Shea KJ. Recognition, neutralization, and clearance of target peptides in the bloodstream of living mice by molecularly imprinted polymer nanoparticles: a plastic antibody. J. Am. Chem. Soc. 2010; 132:6644–6645. [PubMed: 20420394]
36. Hayden O, Lieberzeit PA, Blaas D, Dickert FL. Artificial antibodies for bioanalyte detection-sensing viruses and proteins. Adv. Funct. Mater. 2006; 16:1269–1278.

Europe PMC Funders Author Manuscripts

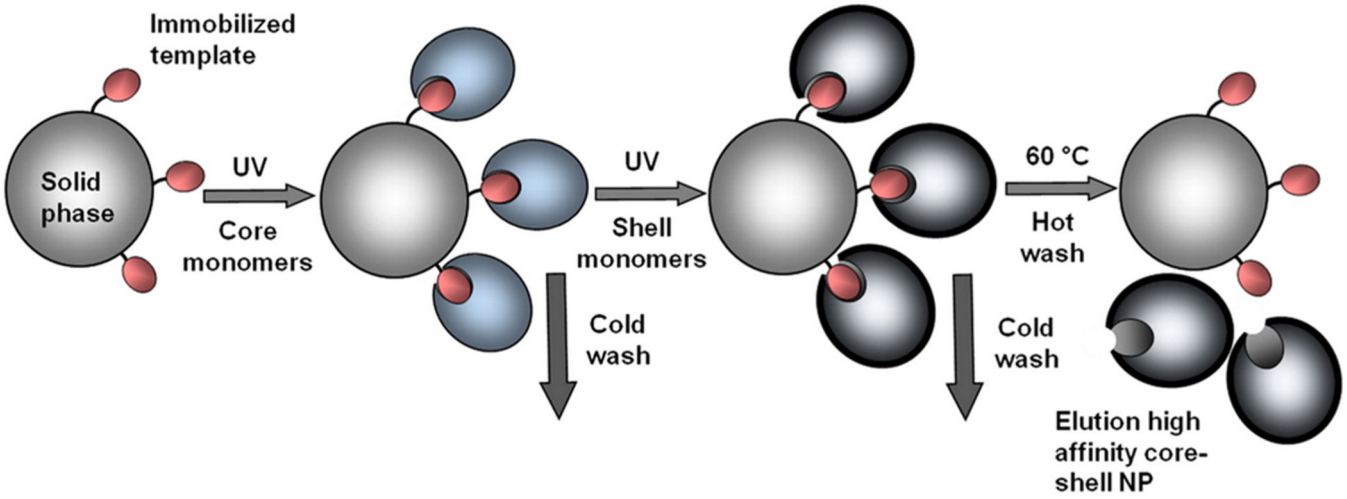

Figure 1.
Schematic representation of the solid-phase method for the synthesis of core–shell MIP NPs

Europe PMC Funders Author Manuscripts

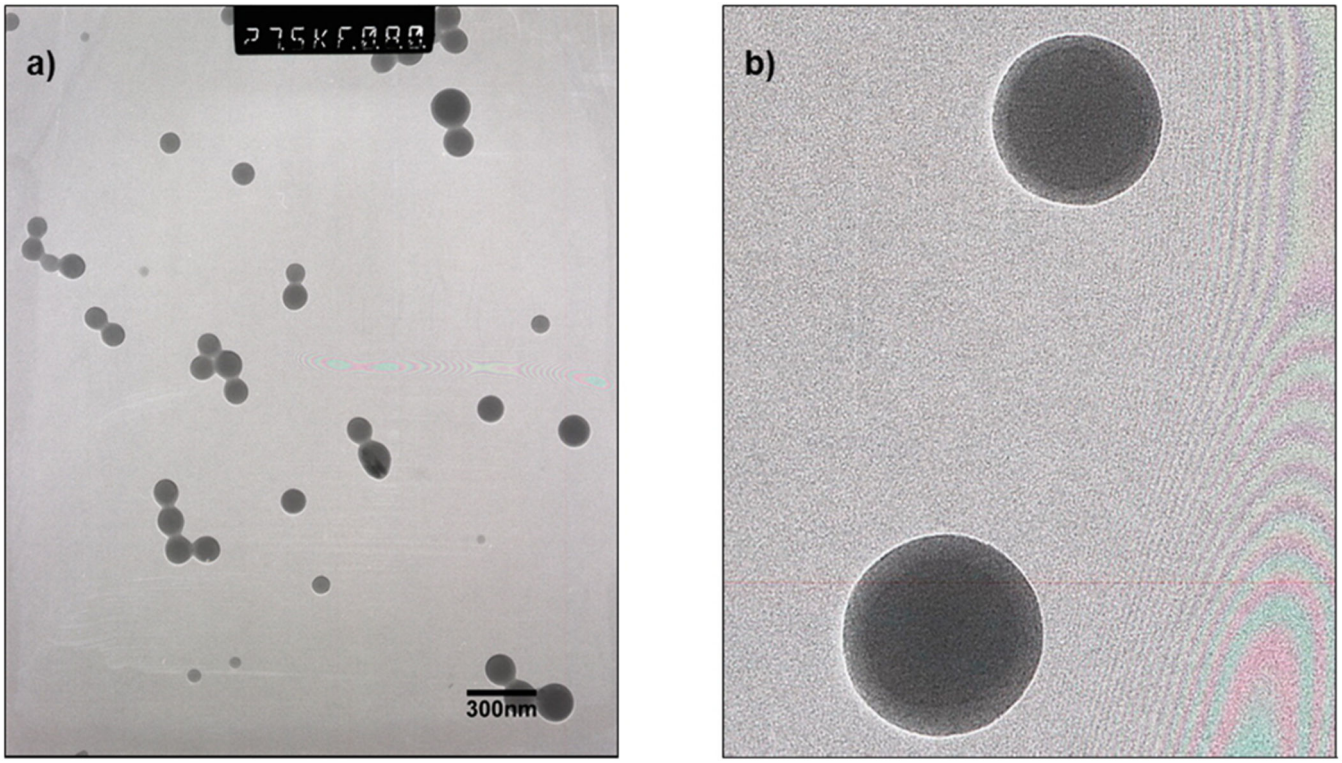

Figure 2.
TEM images of dried, modified MIP nanoparticles (a) at 27.5K× magnification and (b) close up, showing the core–shell structure. Both images are of MIP NPs PEG 1100 75.

Europe PMC Funders Author Manuscripts

Europe PMC Funders Author Manuscripts

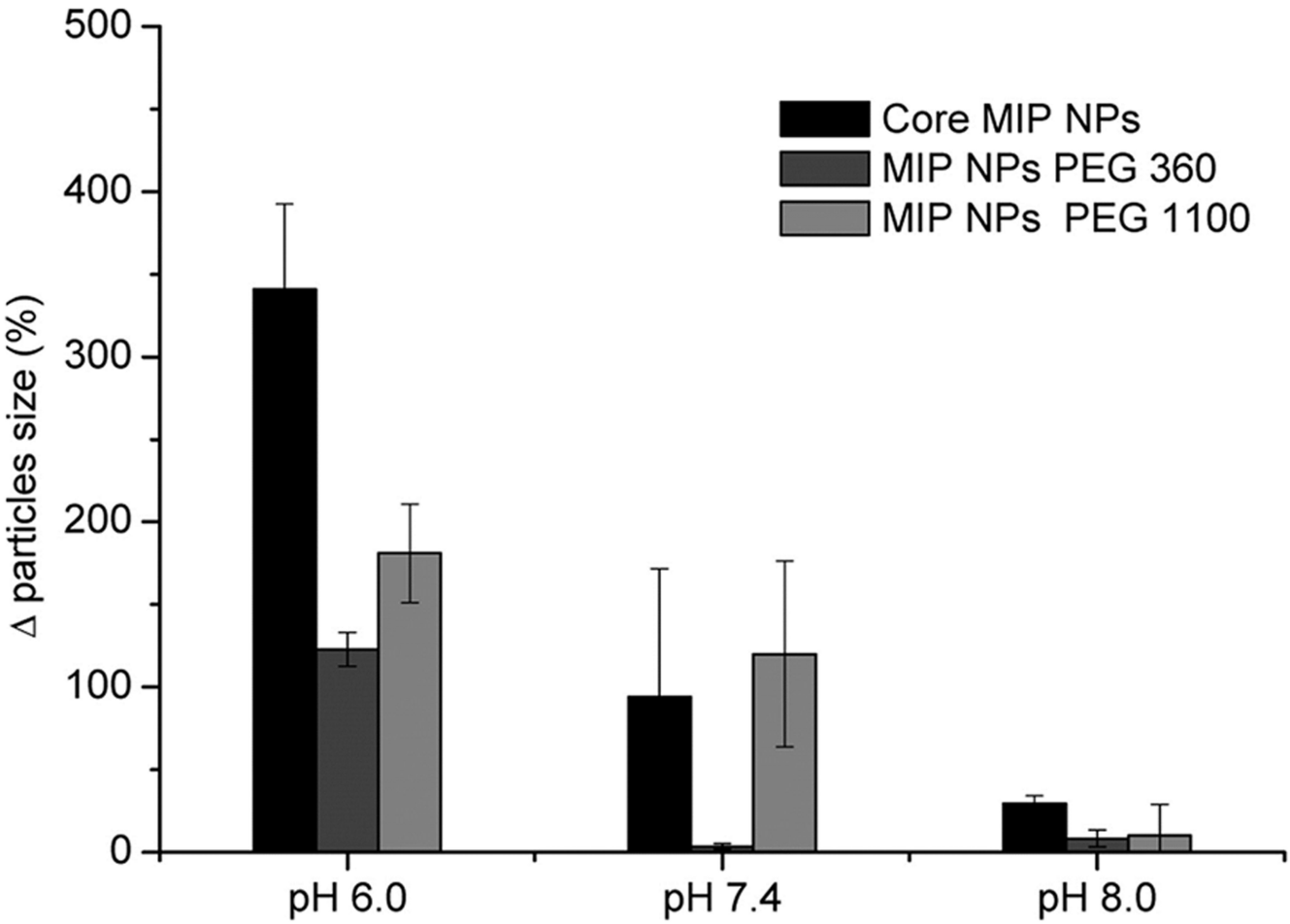

Figure 3.

Changes in the average hydrodynamic diameter of NPs in response to storage in PBS at different pH values. Measurements were performed after 72 h of storage at 20 °C. Error bars indicate standard deviations, n ≥ 3. Core–shell NPs were prepared with either PEG at 10 mg mL^{-1}

Europe PMC Funders Author Manuscripts

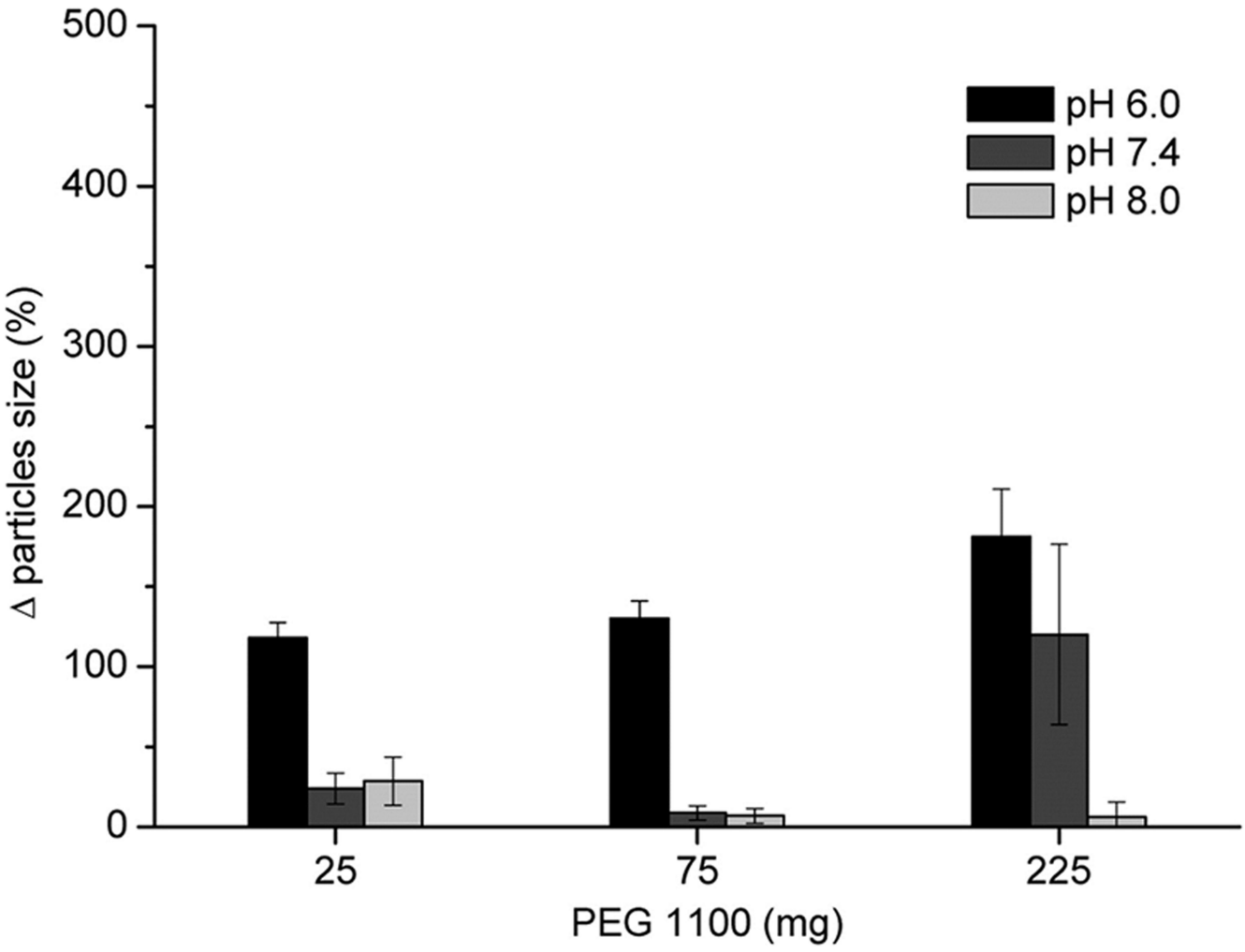

Figure 4.

Changes in the average hydrodynamic diameter of NPs grafted with different amounts of PEG1100 in response to storage in PBS at different pH values. Measurements were performed after 72 h of storage at 20 °C. Different amounts of PEG methacrylate 1100 were dissolved in 7.5 mL of acetonitrile and added to the solid phase containing core NPs before polymerization. Error bars indicate standard deviations, n ≥ 3.

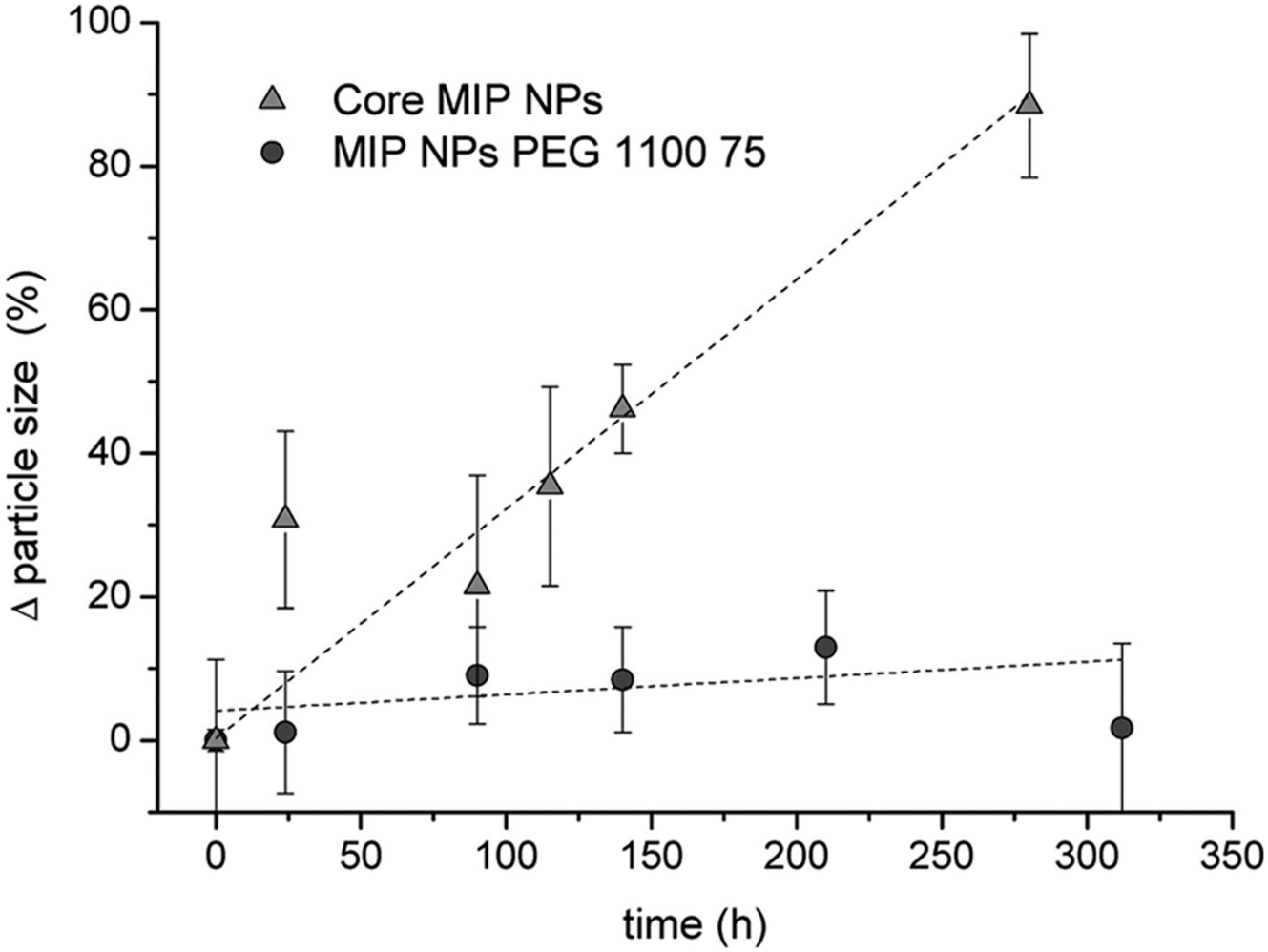

Figure 5.

Storage stability of core MIP NPs and core–shell MIP NPs in deionized water. Points marked as triangles (Δ) and circles (○) indicate the mean values of changes in particle size obtained by DLS measurement as a function of time. Dashed lines (---) indicate linear fits to the data points to help visualize the trend and distinguish both data sets. During the experiment, NPs were stored at 4 °C in order to prevent microbial growth, but measurements were performed at 20 °C. Error bars indicate standard deviations, n ≥ 3.

Europe PMC Funders Author Manuscripts

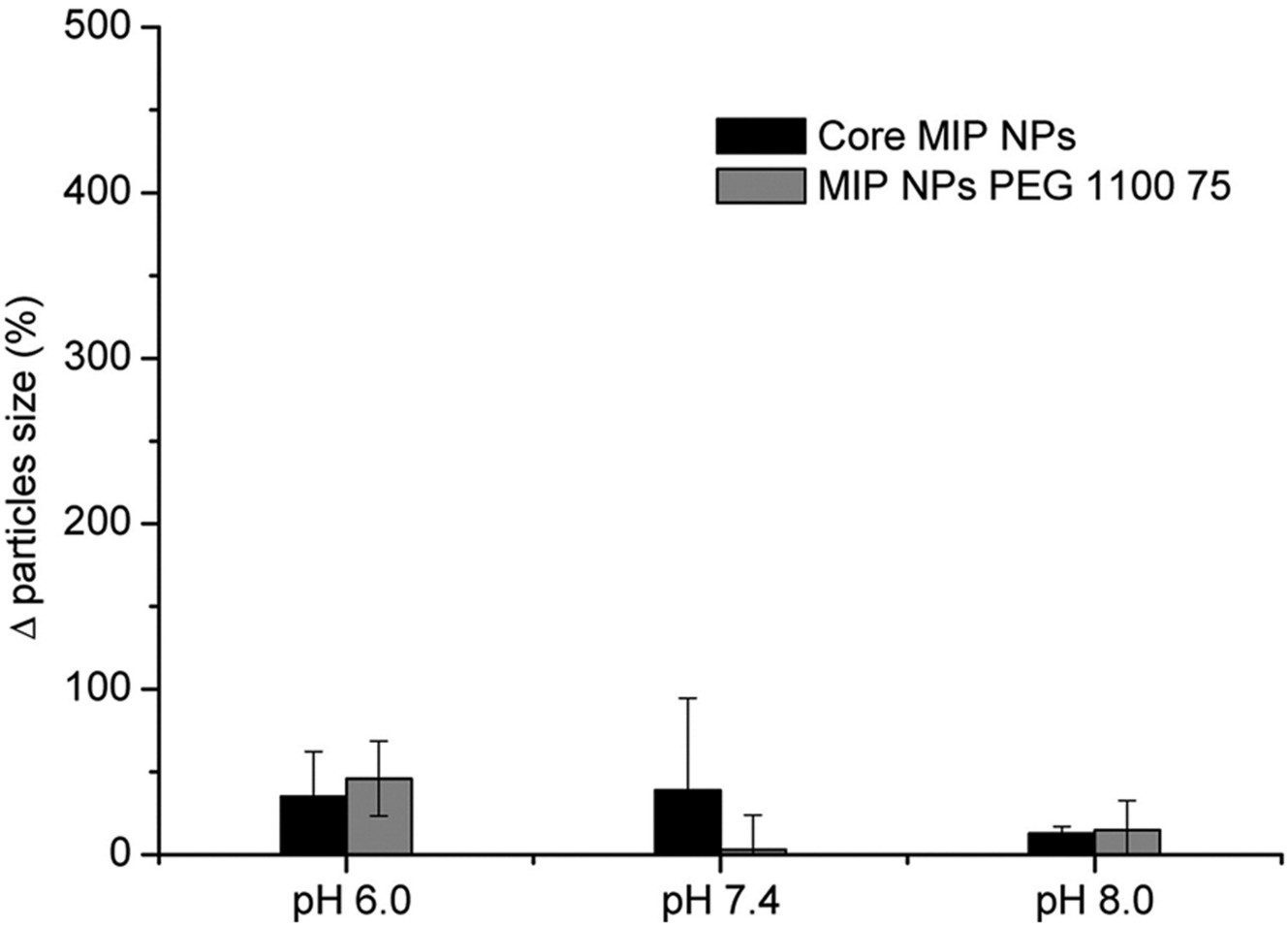

Figure 6.

Changes in the average hydrodynamic diameter of NPs in response to storage in PBS with different pH values in the presence of 8 × 103 ppm BSA. Measurements were performed after 72 h of storage at 20 °C. Error bars indicate standard deviations, n ≥ 3.

Europe PMC Funders Author Manuscripts

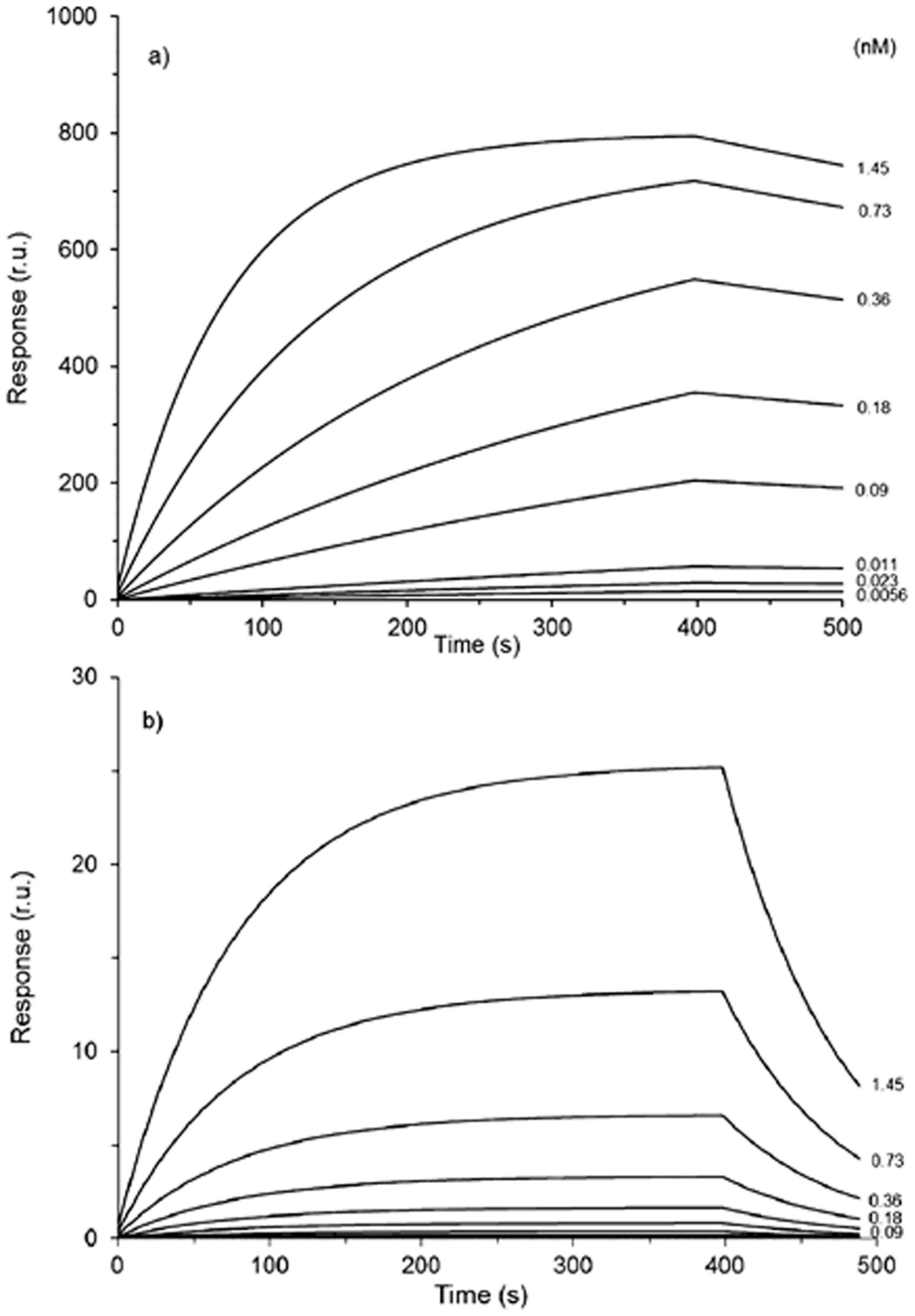

Figure 7.

SPR sensorgrams for core–shell MIP NPs PEG 1100 75 injected (a) onto a specific MEL-coated sensor surface and (b) onto a control DA surface at 25 °C. Solutions of NPs were injected at concentrations ranging from 0.0056 to 1.45 nM as depicted in Figure 7a. Concentrations 0.0056, 0.011, 0.023, and 0.0028 nM are not shown in plot b because no SPR response was obtained for these on the DA surface.

Europe PMC Funders Author Manuscripts

Table 1

Dissociation Constants for the Binding of Core MIP NPs and Core–Shell MIP NP PEG 1100 75 on the Specific Melamine (Mel) Surface and the Nonspecific Desisopropyl Atrazine (DA) Surface at 25 and 36 °C

	MEL surface		DA surface	
	25 °C	**36 °C**	**25 °C**	**36 °C**
core NPs [M]	1.74×10^{-10}	9.27×10^{-10}	2.64×10^{-8}	4.24×10^{-7}
core–shell NPs [M]	0.80×10^{-10}	6.10×10^{-10}	5.39×10^{-8}	1.35×10^{-8}